Extended Tripodal Hydrotris(indazol-1-yl)borate Ligands as Ruthenium-Supported Cogwheels for On-Surface Gearing Motions

Kenichiro Omoto, Menghua Shi, Kazuma Yasuhara, Claire Kammerer, Gwénaël Rapenne

Chemistry–A European Journal | Research Article
doi.org/10.1002/chem.202203483
Chemistry Europe
European Chemical Societies Publishing
www.chemeurj.org

Special Collection

Extended Tripodal Hydrotris(indazol-1-yl)borate Ligands as Ruthenium-Supported Cogwheels for On-Surface Gearing Motions

Kenichiro Omoto,[a] Menghua Shi,[a] Kazuma Yasuhara,[a, b] Claire Kammerer,[c] and Gwénaël Rapenne*[a, c]

Dedicated to Professor J. Fraser Stoddart on the occasion of his 80th birthday.

Abstract: This paper reports the synthesis of ruthenium-based molecular gear prototypes composed of a brominated or non-brominated pentaphenylcyclopentadienyl ligand as an anchoring unit and a tripodal ligand with aryl-functionalized indazoles as a rotating cogwheel. Single crystal structures of the ruthenium complexes revealed that the appended aryl groups increase the apparent diameter of the cogwheel rendering them larger than the diameter of the anchoring units and consequently making them suitable for intermolecular gearing motions once the complexes will be adsorbed on a surface.

Introduction

A wide variety of molecular machines with very different structures and tasks, ranging from intracellular cell transport to energy storage, are found in the biological world.[1] Among them, ATP-synthase[2] is the archetype of a rotary motor which plays a crucial role in the storage of energy in living organisms. This trans-membrane enzyme indeed harnesses energy from a proton gradient across the membrane to drive a unidirectional turbine-like motion leading to the selective conversion of ADP into ATP, to store energy.

The synthesis of miniaturized analogs of biological machines is an active field of research, boosted by the Nobel Prize awarded in 2016 to Prof. J.-P. Sauvage[3] and Sir J. F. Stoddart[4] for their pioneering investigations on mechanically-interlocked molecular machines, and to Prof. B. L. Feringa[5] for the development of a very efficient family of light-fueled motors based on overcrowded alkenes.[6] Since this breakthrough, many synthetic motors with a variety of designs adapted to different media have been reported, powered by light,[7] but also chemical energy sources[8] or electrons.[9]

Once this milestone achieved, it appears highly desirable to exploit these motors to perform more advanced tasks, either by inducing cooperative behaviors within a network of molecules[10] or by developing complex nanomachineries at the single-molecule level. Following a technomimetic[11] approach (i.e. taking macroscopic machines as an inspiration), one possibility is to integrate motors into more sophisticated intramolecular devices such as a nanovehicle[12] or a winch.[13] With a further aim to build functional multimolecular machineries, exploitation of the work provided by a single motor now requires its interconnection with distinct mechanical devices. In the case of surface-bound rotary motors, an interesting strategy consists in the transfer of their rotational motion through a train of gears assembled on a surface.[14]

Indeed, whereas gearing motions can only be performed at the intramolecular level in solution,[15] intermolecular gearing can be achieved in anisotropic media[16] where it becomes possible to precisely control and maintain the distance between molecular cogwheels. In particular, the transfer of rotational motion has been successfully demonstrated within systems of meshed star-shaped molecules anchored on a surface.[17] In such experiments, the tip of a scanning tunneling microscope (STM) is used to build a train of gears by initially positioning the single-molecule cogwheels with appropriate interlocking distance, and then as a source of mechanical energy to induce the rotation of the first cogwheel. Propagation of the motion

[a] Dr. K. Omoto, M. Shi, Dr. K. Yasuhara, Prof. Dr. G. Rapenne
Division of Materials Science
Nara Institute of Science and Technology
8916-5 Takayama, Ikoma, 630-0192(Japan)
E-mail: gwenael-rapenne@ms.naist.jp

[b] Dr. K. Yasuhara
Center for Digital Green-innovation
Nara Institute of Science and Technology
8916-5 Takayama-cho, Ikoma, 630-0192 (Japan)

[c] Dr. C. Kammerer, Prof. Dr. G. Rapenne
CEMES, Université de Toulouse, CNRS
29, rue Marvig, 31055 Toulouse (France)
Homepage: https://www.cemes.fr/rapenne

Supporting information for this article is available on the WWW under https://doi.org/10.1002/chem.202203483

Special Collection This publication is part of a Special Collection on aromatic chemistry in collaboration with the "19th International Symposium on Novel Aromatic Compounds (ISNA-19)".

through the gears is evidenced by comparing successive STM images.

Only a few star-shaped molecules have been studied on surface as molecular gears like the penta(*p*-*tert*-butylphenyl)-(*p*-*tert*-butylpyrimido)benzene exploited as a six-teeth cogwheel by Moresco et al.[17] In this pioneering work, when a single molecule was moved laterally with the STM tip along an island of the same hexaarylbenzene molecules on Cu(111), rotation of the molecule was evidenced on successive STM images, similarly to a rack and pinion. Unfortunately, when working on a pair of molecules, all attempts to transfer rotation from one to the next were unsuccessful because diffusion of the molecules was more favorable.[18] An anchoring group to pin individual cogwheels at precise interlocking distances is thus the key for intermolecular gearing. This concept was applied to the same molecule, which was next mounted on a single Cu adatom acting as an atomic scale axle to allow a precise positioning of the cogwheels on the Pb(111) surface.[19] This resulted in the transfer of a rotational motion from one molecule to the next but the transfer of rotation to a third molecule failed due to the fragility of the supramolecular anchoring structure. This progress towards on-surface intermolecular gearing underlines the importance to integrate an anchoring subunit in the molecular design.

Another anchoring strategy exploited the strong interaction between the Au(111) surface and the radical state of pentaarylcyclopentadienyl cogwheels, generated by an homolytic cleavage of a brominated precursor upon on-surface deposition by sublimation. In collaboration with the group of Moresco,[20] we obtained for the first time the transfer of a gearing motion up to three interlocked molecules. Unfortunately, this strategy is not suitable to build trains of gears of controlled shape and length since the anchoring position is random and once anchored, the radical species proved impossible to be repositioned, which is a key issue to build a train of gears with a controlled arrangement.

A promising alternative strategy relies on the use of a metallo-organic rotation axle, in which the ligand provides tight anchoring on the surface through specific functional groups with the metal ion acting as a ball bearing. In this regard, a series of ruthenium complexes were recently reported with a thioether-functionalized hydrotris(indazol-1-yl)borate ligand[21] acting as a tripodal platform for pentaarylcyclopentadienyl cogwheels.[22] In order to increase the diversity of functional molecular gear systems and ultimately implement gearing ratios in surface-bound nanomachineries, we currently aim at exploring the mechanics of cogwheel prototypes with shapes differing from the 6- and 5-pointed stars exemplified up to now.

In a previous work,[23] a ruthenium-based molecular motor (molecule **1** represented Figure 1) incorporating a three-blades rotating subunit (in blue) was successfully adsorbed on a Au(111) surface through a penta(*p*-bromophenyl)cyclopentadienyl ligand acting as anchoring subunit (in green). During this study, it has also been shown this tripodal ligand allows a precise repositioning of the complexes by lateral manipulation with the STM tip. This possibility to

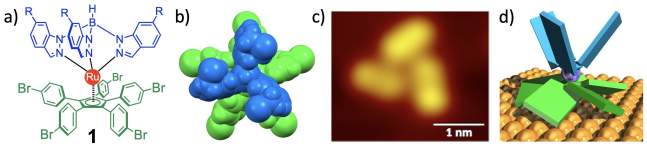

Figure 1. a) Chemical structure of the ruthenium complex **1** used in our previous study,[23] b) its molecular modeling (top view) showing the left-handed twisting of the tripodal ligand (the ethyl groups are omitted for clarity) c) the STM image of **1** on Au(111) at 77 K and d) a paddle-like representation of the ΛΛ molecule showing the left-handed twisting of the lower ligand (in green) and the resulting left-handed twisting of the upper tripodal ligand (in blue).

reposition a molecule, after its random deposition on the surface, is a unique feature of this anchoring unit which opens perspectives to build linear trains of molecular gears.

Under the influence of an electric field induced by the STM tip or of inelastic tunneling electrons, individual molecules undergo unidirectional rotation of the hydrotris(indazol-1-yl)borate upper subunit with a direction controlled by the helicity of the motor on surface. Indeed, this complex is not chiral in solution, but upon adsorption on the surface, twisting of the penta(*p*-bromophenyl)cyclopentadienyl subunit occurs in a left- or a right-handed manner with equal probability. This helicity of the bottom ligand (in green on Figure 1) then controls the chirality of the upper tripodal hydrotris(indazol-1-yl)borate ligand (in blue on Figure 1) in a homochiral fashion. As a consequence, two enantiomers (ΔΔ and ΛΛ) of the ruthenium complex are observed on the surface in equal proportions.

Due to the three-fold symmetry of the rotating subunit, this type of architecture appears very attractive as a candidate for novel gearing systems involving a metallo-organic anchoring subunit which can be repositioned at will on the surface. Also, the helical structure of these complexes on the surface will allow to gain insight into the influence of cogwheel helicity on mechanics at the molecular scale. Indeed, to allow for disrotatory motions expected in a train of gears, it is envisioned to position a right-handed molecule (which rotates anticlockwise) next to a left-handed molecule (which rotates clockwise). Experimental on-surface studies and comparison with homochiral trains of gears will thus allow to verify the assumption that a chirality inversion in the successive cogwheels is helpful in order to transfer rotation in intermolecular gearing systems.

Unfortunately, in ruthenium complex **1**, the diameter of the rotating 3-teeth cogwheel is too small (12.2 Å, in blue) compared to the diameter of the anchoring pentaarylcyclopentadienyl subunit (14.5 Å, in green), which makes the transfer of rotation from one cogwheel to the next extremely difficult to envision. To favor interlocking between neighboring cogwheels, two strategies depicted on Figure 2 were explored to increase the diameter of the rotating subunit as compared to that of the anchoring subunit.

Herein we report the synthesis of two new extended tripodal ligands incorporating aryl groups at the 5-position of the indazole, which clearly enlarged their diameter. As an

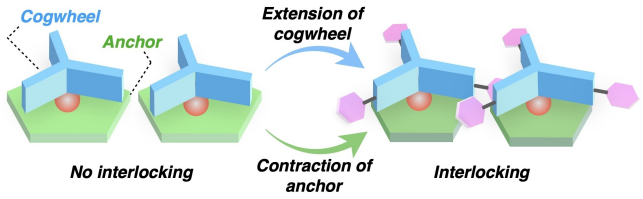

Figure 2. Conceptual representation of our two strategies to obtain a molecular structure which could allow the interlocking of two neighboring cogwheels (in blue) by extension of the cogwheel and contraction of the anchor subunit (in green) and ultimately make possible a transfer of rotation from one cogwheel to the next.

alternative strategy, the diameter of the anchoring subunit was reduced and the corresponding complexes involving the smaller non-brominated pentaphenylcyclopentadienyl ligand are also reported. X-ray structures of all ruthenium complexes have been obtained which allowed us to determine the best candidates for on-surface intermolecular gearing studies.

Results and Discussion

Design of the ruthenium complexes with different diameters of cogwheel and anchor

We designed four organometallic molecular gears prototypes exhibiting different diameters for the cogwheel and anchoring group (**Ga-Br**, **Gb-Br**, **Ga-H** and **Gb-H**). They have been obtained by combination of two distinct hydrotris(indazol-1-yl)borate ligands functionalized with different aryl groups on the 5-position of the indazole as cogwheels and two pentaphenylcyclopentadienyl ligands substituted or not by bromine atoms on para positions as anchors (Scheme 1).

For the tripodal cogwheels, molecular modelling studies[24] showed that the 5-position of indazole is the most efficient to increase the diameter of the hydrotris(indazol-1-yl)borate ligand, since the new C–C bonds located at this position are oriented perpendicular to the B–Ru rotation axis in the ruthenium complex. Accordingly, two tripodal ligands with

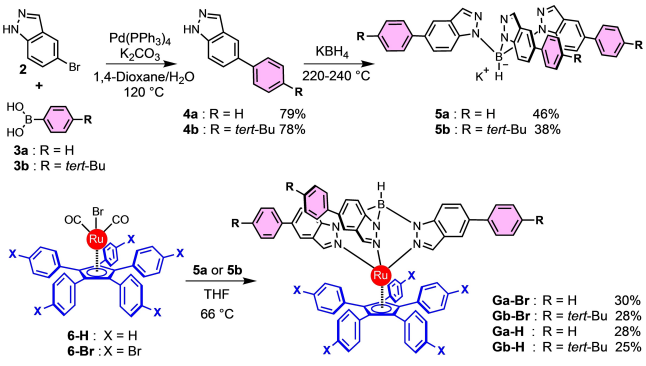

Scheme 1. Preparation of the four ruthenium complexes with the extended tripodal hydrotris(indazol-1-yl)borate ligands as Ru-supported cogwheels.

phenyl (R=H) and 4-(*tert*-butyl)phenyl (R=*tert*-Bu) groups on indazole 5-positions were designed to give rise to extended cogwheels with increasing diameter.

As anchoring subunit, we exploited the penta(*p*-bromophenyl) cyclopentadienyl ligand already used in our previous studies on molecular motor **1**, because it showed very efficient anchoring properties[23] on the Au(111) surface combined with the ability to be repositioned on such surface by STM lateral manipulation. With the idea to reduce the diameter of the anchoring unit, we also prepared complexes with the non-brominated pentaphenylcyclopentadienyl ligand, which is expected to have a sufficient interaction with the metal surface to immobilize the gear as it has been observed in other studies on similar compounds.[20]

Synthesis of the functionalized tripodal ligands

The two extended tripodal ligands incorporating 5-phenyl-1*H*-indazole (R=H, **5a**) or 5-(4-*tert*-butylphenyl)-1*H*-indazole (R=*tert*-Bu, **5b**) fragments were prepared in two steps from 5-bromo-1*H*-indazole **2**, according to Scheme 1. First, **2** was reacted with the appropriate aromatic boronic acid **3a** (R=H) or **3b** (R=*tert*-Bu) via a Suzuki-Miyaura coupling to yield the corresponding aryl-substituted indazoles **4a** (R=H) or **4b** (R=*tert*-Bu). After heating with KBH_4 without any solvent, the two expected hydrotris(indazol-1-yl)borates ligands **5a** (R=H) and **5b** (R=*tert*-Bu) were obtained as potassium salts. The formation of each species was confirmed by NMR spectroscopy and ESI-TOF mass spectrometry (Figures S1–S6). As reported by S. Trofimenko and coworkers,[25] it must be noted that the temperature of the reaction controls the number of boron substitutions. Indeed, a lower temperature (around 150 °C) usually gives mainly the bipode derivative whereas a higher temperature (around 280 °C) will allow the formation of the tetrapode.

Concerning the regiochemistry of the reaction, this is well established from previous studies[26] that the interplay of steric and electronic factors tilts exclusively in favor of the formation of the hydrotris(indazol-1-yl)borate ligand, in which the boron atom is bound to the more hindered nitrogen atom located next to the ring fusion. The Tp^{4Bo} isomer is thus obtained as a sole product and no trace of the Tp^{3Bo} compound is observed. As a consequence, these ligands are sterically hindered around the boron atom but not on the coordination side. This regiochemistry was confirmed by our X-ray studies (see below).

Synthesis of the ruthenium complexes

The target ruthenium complexes were prepared by substitution of the bromide ligand and CO displacement by heating precursors **6-Br** or **6-H** with 2 equivalents of the potassium salt of the appropriate tripodal ligands **5a** or **5b** in anhydrous and degassed THF under reflux (Scheme 1). By combining the different ruthenium precursors and tripodal ligands, a total of four different ruthenium complexes were obtained: **Ga-Br** (X=Br, R=H), **Gb-Br** (X=Br, R=*tert*-Bu), **Ga-H** (X=H, R=H) and **Gb-**

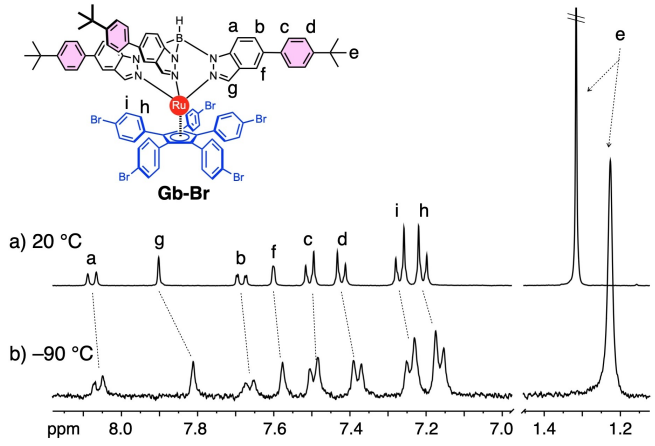

Figure 3. ^{1}H NMR spectra of complex **Gb-Br** measured at a) 20 °C and b) −90 °C in CD_2Cl_2 (400 MHz).

H (X=H, R=*tert*-Bu). The ligand exchange reaction proceeded gradually to give the ruthenium complexes along with some green byproducts. After purification by SiO_2 column chromatography and subsequent reprecipitation or recrystallization from dichloromethane/methanol or chloroform/methanol, the desired ruthenium complexes were isolated in 25 to 30% yield as orange solids. All ruthenium complexes were characterized by NMR spectroscopy, ESI-TOF mass spectrometry and single crystal X-ray structural analyses as follows. All the data are given in the experimental part and Supporting Information (Figure S7–S22).

NMR spectroscopy of the ruthenium complexes

For a detailed discussion, we have selected the ^{1}H NMR spectra of **Gb-Br** (X=Br, R=*tert*-Bu) as a representative complex. Figure 3a shows the ^{1}H NMR spectrum of **Gb-Br** in CD_2Cl_2 at 20 °C displaying signals assignable to the protons of aryl-substituted indazole units around 8.1–7.3 ppm (a–d, f–g) and those of *p*-bromophenylene units around 7.3–7.0 ppm (h and i), respectively.

The integral ratios of these peaks are consistent with the formation of a 1:1 heteroleptic complex composed of the tripodal ligand and the penta(*p*-bromophenyl)cyclopentadienyl ligand. Notably, the three indazole fragments were observed to be equivalent, although there is a symmetry discrepancy between the tripodal ligand (three-fold symmetry) and the penta(*p*-bromophenyl)cyclopentadienyl ligand (five-fold symmetry). This result indicates that the ruthenium complex undergoes an intramolecular free rotational motion along the Cp–Ru bond as rotation axle on the ^{1}H NMR timescale at 20 °C, resulting in the equivalence of the three indazole fragments. To discuss temperature dependency of this rotational motion, ^{1}H NMR of complex **Gb-Br** was also measured at −90 °C in CD_2Cl_2 (Figure 3b). A similar spectrum was observed with the same number of signals appearing at a higher field, thus indicating that free intramolecular rotation is maintained even at −90 °C. These results suggest that the ruthenium ion in such complexes works as an ideal ball bearing between both ligands, that leads to a smooth intramolecular rotation around the Ru–Cp bond.

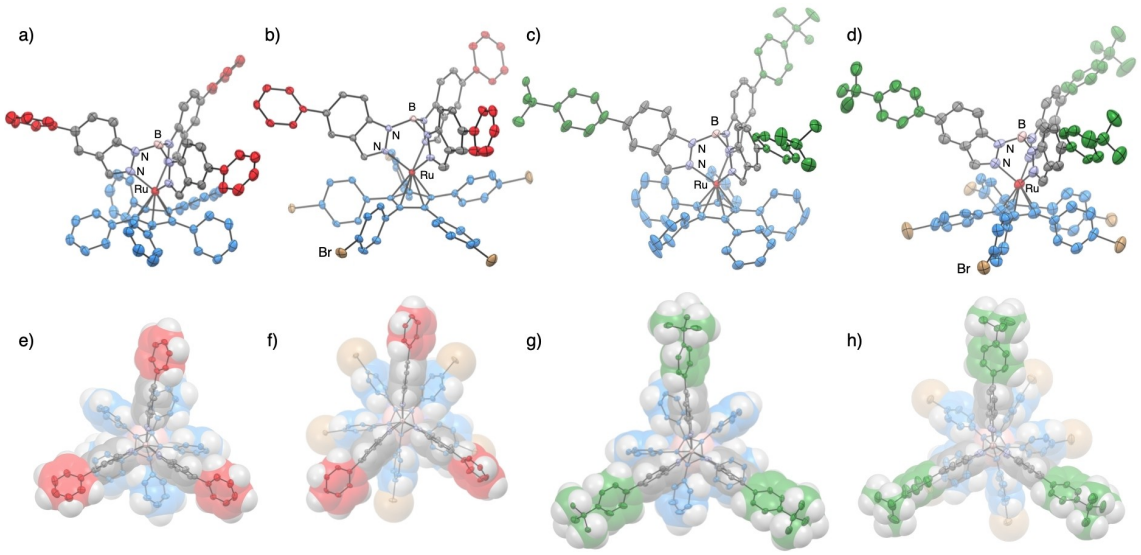

Figure 4. ORTEP representation of the crystal structures of a, e) **Ga-H** (X=H, R=H), b, f) **Ga-Br** (X=Br, R=H), c, g) **Gb-H** (X=H, R=*tert*-Bu) and d, h) **Gb-Br** (X=Br, R=*tert*-Bu). Side views (a–d) and top views (e–h). Phenyl and *tert*-butylphenyl groups of the extended tripodal ligands are colored in red and green, respectively. In the cases of **Ga-H**, **Ga-Br** and **Gb-Br**, ones of the crystallographically non-equivalent structures are described. Hydrogen atoms in ORTEP representation and molecules of solvent have been omitted for clarity. The ellipsoids are drawn at the 50% probability level.

Single crystal structures of the ruthenium complexes

Crystals suitable for X-Ray diffraction of the four ruthenium complexes (**Ga-Br**, **Gb-Br**, **Ga-H** and **Gb-H**) were grown by slow diffusion of methanol over a dichloromethane or chloroform solution. The structures were resolved by using single-crystal X-ray diffraction analysis (Figure 4). From these crystal structures, we confirmed the formation of heteroleptic complexes composed of an aryl-substituted tripodal ligand and a pentaphenyl cyclopentadienyl ligand, as discussed in the above-described structural analyses using NMR spectroscopy and ESI-TOF mass spectrometry. We also confirmed the expected regiochemistry of the tripodal ligand with the exclusive formation of the hydrotris(indazol-1-yl)borate isomer, displaying the boron atom bound to the nitrogen located next to the ring fusion. These crystal structures revealed that the diameter of the tripodal ligand in each complex was indeed extended by addition of the terminal aryl group on the indazole 5-position and that all cogwheel subunits are larger in diameter than the corresponding anchoring subunit (Figure 4e–h). In the crystals, the ruthenium complexes are packed via weak intermolecular interactions such as CH–π and van der Waals interactions. Tripodal ligands showed intermolecular packing with a more or less distorted deviation from the 3-fold symmetry. Instead of ideal 120° angles between indazole rings, we observed angles in the range of 92 to 140°. Interestingly, the three-fold aryl-substituted tripodal ligands of each complex in the crystal intermolecularly mesh with another like in a train of gears (molecular packing of complex **Ga-Br** is shown in Figure 5 as a representative example).

As mentioned above, the ratio between the diameter of the cogwheel (tripodal ligand) defined as $D_{cogwheel}$ and the diameter of the anchoring subunit (pentaphenylcyclopentadienyl ligand) defined as D_{anchor} must be as large as possible to allow an efficient interlocking of the cogwheels to form trains of molecular gears, while avoiding negative interactions between the anchoring units. The diameter of the anchoring ligand and the cogwheel have been measured in each complex from their single crystal structures according to the Figure 6. The respective values given in Table 1 are the measured diameters of the circumscribed circles consisting of the outermost atoms of the pentaphenylcyclopentadienyl ligand (D_{anchor}) and those of the tripodal ligand ($D_{cogwheel}$) in each complex. For comparison, the values for ruthenium complex **1** composed of tripodal ligand without peripheral aryl group are also given. D_{anchor} of each pentaphenylcyclopentadienyl ligand was evaluated to be 12.8 Å (with X=H) and 14.5 Å (with X=Br), illustrating that the size of the anchoring unit can be tuned by varying the peripheral atoms. $D_{cogwheel}$ of complexes **Ga-X** and **Gb-X** were evaluated to be as large as 20.6–21.2 Å and 25.2–25.4 Å, respectively, which are drastically larger than the cogwheel in complex **1** (12.2 Å).

This result illustrates that the diameters of the tripodal ligands were successfully increased by their functionalization at the 5-position with aryl groups. Notably, ratio of the diameters of ligands ($D_{cogwheel}/D_{anchor}$) increased from 0.8 in molecular motor **1** to 1.5–2.0 in the series of the new ruthenium complexes described here. Such a significant increase in the ratio suggests that the cogwheels can now interlock intermolecularly with each other without any undesired steric hindrance between the anchoring ligands. This was not possible in **1** because the anchoring subunit prevented the interlocking of cogwheels due to its larger diameter.

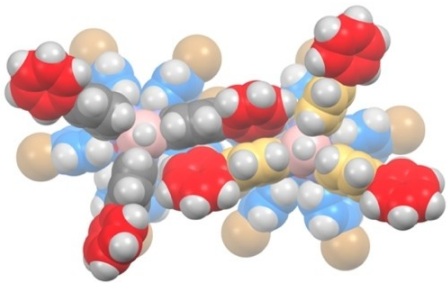

Figure 5. Molecular packing of complex **Ga-Br** (X=Br, R=H) with two crystallographically inequivalent molecules, showing that adjacent tripodal ligands intermesh like two consecutive gears.

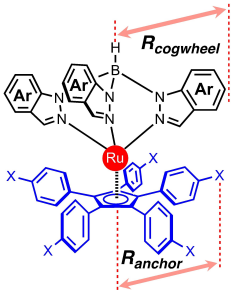

Figure 6. Procedure to determine the key parameters named R_{anchor} and $R_{cogwheel}$ are given in the Table 1. They were determined as the measured radii from the corresponding X-ray structures. The hydrogen atoms were included in the measurement even if they have been introduced by calculation in the X-ray structure determination.

Table 1. Diameter of the anchoring ligands (D_{anchor}) with or without bromine and those of the cogwheels ($D_{cogwheel}$) with or without *tert*-butyl groups and the corresponding ratio ($D_{cogwheel}/D_{anchor}$). Diameters have been measured from the X-ray structures of the four ruthenium complexes as explained below.

Ruthenium complex	1	Ga-H	Ga-Br	Gb-H	Gb-Br
		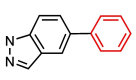	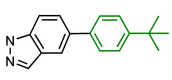		
X	Br	H	Br	H	Br
$D_{cogwheel}$ [Å][a]	12.2[c]	20.6	21.2	25.4	25.2
D_{anchor} [Å][b]	14.5	12.8	14.5	12.8	14.5
Ratio	0.8	1.6	1.5	2.0	1.7

[a] The radius of the anchor (R_{anchor}) is determined as the average distance between the 5 outermost atoms (Br or H atoms) and the centroid of the cyclopentadienyl fragment. [b] The radius of the cogwheel ($R_{cogwheel}$) is determined as the radius of the circumscribed circles of the triangles composed of the outermost H atoms at the 5-position of the three indazoles. [c] This value was measured from previous crystal structures of analog complexes bearing this tripodal ligand.[13a]

Conclusion

In this work, we designed and synthesized ruthenium-based molecular gears composed of a pentaphenylcyclopentadienyl ligand as an anchoring subunit and a tripodal ligand with aryl-extended indazoles as a cogwheel. Each complex was characterized by NMR spectroscopy, ESI-TOF mass spectrometry and X-ray crystallography. ^{1}H NMR spectra showed that such complexes exhibit free intramolecular rotational motion on the time scale of ^{1}H NMR in solution, revealing that the Ru-Cp bond of the complexes works as an ideal axle to realize smooth intramolecular rotation. Single crystal structure of each complex revealed that aryl groups on the hydrotris(indazol-1-yl)borate ligands increase their apparent diameter, rendering them drastically larger than the diameter of the pentaphenylcyclopentadienyl anchoring subunits. Thus, the here described ruthenium complexes with such extended tripodal ligand are expected to behave as cogwheels in intermolecular gearing systems working on metal surfaces, where tripodal ligands of linearly arranged complexes can interlock in each other to realize a desired efficient propagation of rotational motion. STM studies are underway to adsorb these molecules on a Au(111) surface and study the possibility to transfer rotary motion through a pair of molecules, either homochiral or heterochiral. Once it will be established between two consecutive molecules, the formation of a longer train of gears will be explored.

Experimental Section

General methods: Synthetic procedures were carried out under dry N_2 atmosphere, unless otherwise specified. All reagents and solvents were purchased at the highest commercial quality available and used without further purification, unless otherwise stated. Anhydrous tetrahydrofuran, 5-bromo-1*H*-indazole (**2**), chloroform, 1,4-dioxane, methanol and 4-(*tert*-butyl)phenylboronic acid (**3 b**) were purchased from FUJIFILM Wako Pure Chemical Corporation. $Pd(PPh_3)_4$ was purchased from Sigma Aldrich. Dichloromethane was purchased from Nacalaitesque. Phenylboronic acid (**3 a**) was purchased from TCI. **6-H**[27] and **6-Br**,[28] were prepared according to the literature procedures. Silica gel column chromatography and thin-layer chromatography (TLC) were performed using CHROMATOREX PSQ 100B and Merck silica gel 60 (F254) TLC plates, respectively. The ESI-TOF mass spectrometry was performed using JEOL AccuTOF JMS-T100LC with sodium trifluoroacetate as an internal standard. CEM Discover SP was used for reactions using a microwave irradiator. Single crystal X-ray crystallographic analysis was performed using a Rigaku VariMax RAPID (1.2 kW) diffractometer with confocal mirror optics MoKα radiation. Single crystals for diffraction measurements were mounted with epoxy resin on a glass fiber, the temperature of which was controlled using a nitrogen gas-flow. Crystal structures were solved with SHELXT[29] and L.S. refinement was performed with SHELXL[30] within Olex2 GUI.[31] Hydrogen atoms were refined using the riding model. ^{1}H- and ^{13}C NMR spectra were recorded on a JEOL JNM-ECA600 (600 MHz for ^{1}H; 150 MHz for ^{13}C) spectrometer, a JEOL JNM-ECZ500 (500 MHz for ^{1}H; 126 MHz for ^{13}C) spectrometer, or a JEOL JNM-ECX400P (400 MHz for ^{1}H; 100 MHz for ^{13}C) spectrometer at a constant temperature of 293 K unless otherwise specified. Tetramethylsilane (TMS) was used as an internal reference for ^{1}H and ^{13}C NMR measurements in $CDCl_3$ and d_6-DMSO respectively. A residual peak of solvent was used as an internal reference for ^{1}H NMR measurements in CD_2Cl_2. Chemical shifts (δ) are reported in ppm. Coupling constants (J) are given in Hz and the following abbreviations have been used to describe the signals: singlet (s); broad singlet (br. s); doublet (d); triplet (t); multiplet (m). The signal of the BH proton in **5 a**, **5 b**, **Ga-Br**, **Gb-Br**, **Ga-H** and **Gb-H** have not been observed due to the quadrupolar relaxation of the proton coupled with the nuclear spin of the boron atom.[32]

Potassium hydrotris(5-phenylindazol-1-yl)borate (5 a): 5-Phenyl-1*H*-indazole (**4 a**) (758 mg, 3.90 mmol, 2.1 equiv.) and KBH_4 (98.5 mg, 1.83 mmol, 1.0 equiv.) were ground up in a mortar and placed in a test tube sealed with a rubber septum. After replacing of the inner gas by dry N_2, the mixture was heated at 230 °C for 3 h under neat conditions. After cooling down to room temperature, remaining unreacted compound **4 a** was removed under vacuum to obtain a dark brown solid as a residue. The resulted dark brown product was sequentially washed with toluene, *n*-hexane and CH_2Cl_2 to obtain compound **5 a** (377 mg, 0.60 mmol) as a colorless solid in a 46% yield. ^{1}H NMR (400 MHz, d^6-DMSO/TMS): δ = 7.98 (s, 3H), 7.88 (br. s, 3H), 7.63 (d, J = 7.6 Hz, 6H), 7.41 (dd, J = 7.6, 7.6 Hz, 6H), 7.32 (dd, J = 1.4 Hz, 9.0 Hz, 3H), 7.29–7.22 (m, 6H); ^{13}C NMR (100 MHz, d^6-DMSO/TMS): δ = 143.3, 141.5, 132.6, 130.8, 128.6, 126.5, 126.1, 125.0, 123.1, 117.2, 113.1. HR-MS (ESI, negative mode) calcd. for $[C_{39}H_{28}BN_6]^-$: 591.2475, found 591.2538.

Potassium hydrotris[5-(4-*tert*-butylphenyl)-indazol-1-yl]borate (5 b): 5-(*tert*-4-Butylphenyl)-1*H*-indazole (**4 b**) (900 mg, 3.60 mmol, 3.4 equiv.) and KBH_4 (56.6 mg, 1.05 mmol, 1.0 equiv.) were ground up in a mortar and placed in a test tube sealed with a rubber septum. After replacing the inner gas by dry N_2, the mixture was heated at 230 °C for 6 h under neat conditions. After cooling down to room temperature, remaining unreacted compound **4 b** was removed under vacuum to obtain a dark brown solid as a residue. The resulted dark brown product was sequentially washed with toluene and *n*-hexane to obtain compound **5 b** (316 mg, 0.40 mmol) as a colorless solid in a 38% yield. ^{1}H NMR (500 MHz, d^6-DMSO/TMS): δ = 7.96 (s, 3H), 7.84 (br. s, 3H), 7.56 (d, J = 8.0 Hz, 6H), 7.42 (d, J = 8.5 Hz, 6H), 7.29 (dd, J = 1.5, 9.0 Hz, 3H), 7.21 (d, J = 8.5 Hz, 3H), 1.30 (s, 27H); ^{13}C NMR (126 MHz, d^6-DMSO/TMS): δ = 148.6, 143.4, 138.8, 132.7, 130.9, 126.3, 125.6, 125.2, 123.2, 117.0, 113.3, 34.2, 31.2. HR-MS (ESI, negative mode) calcd. for $[C_{51}H_{52}BN_6]^-$: 759.4355, found: 759.4304.

Ruthenium complex with X=Br, R=H (Ga-Br): A mixture of compound **5 a** (100 mg, 0.16 mmol, 2.1 equiv.) and **6-Br** (83.6 mg, 78 μmol, 1.0 equiv.) were placed in a two-necked flask. After adding anhydrous and degassed THF (4 mL), the mixture was refluxed for 68 h under N_2 atmosphere. After cooling down to room temperature, the solvent was removed by evaporation under reduced pressure. The crude product was purified by column chromatography (SiO_2, *n*-hexane/CH_2Cl_2 = 4/1). After reprecipitation from a $CHCl_3$/MeOH and washing with *n*-hexane, compound **Ga-Br** (36.0 mg, 24 μmol) was obtained as an orange solid in a 30% yield. ^{1}H NMR (400 MHz, $CDCl_3$/TMS): δ = 8.07 (d, J = 8.8 Hz, 3H), 7.89 (s, 3H), 7.67 (dd, J = 1.6, 8.8 Hz, 3H), 7.62 (br. s, 3H), 7.57 (d, J = 7.6 Hz, 6H), 7.41 (dd, J = 7.6, 7.6 Hz, 6H), 7.31 (t, J = 7.4 Hz, 3H), 7.21 (AA'BB', 20H); ^{13}C NMR (150 MHz, $CDCl_3$/TMS): δ = 142.9, 141.6, 140.9, 133.8, 133.7, 133.6, 128.7, 127.2. 127.2, 127.1, 126.6, 126.5, 123.5, 118.0, 111.8, 88.0. HR-MS (ESI, positive mode) calcd. for $[C_{74}H_{48}BBr_5N_6Ru]^+$: 1531.8983, found 1531.9050.

Ruthenium complex with X=Br, R=*tert*-Bu (Gb-Br): A mixture of compound **5 b** (125 mg, 0.16 mmol, 2.1 equiv.) and **6-Br** (84.3 mg, 0.078 mmol, 1.0 equiv.) were placed in a two-necked flask. After adding anhydrous and degassed THF (4 mL), the mixture was refluxed for 10 days under N_2 atmosphere. After cooling down to room temperature, the solvent was evaporated under reduced pressure. The crude product was purified by column chromatog-

raphy (SiO_2, *n*-hexane/CH_2Cl_2 = 1/1). After recrystallization from CH_2Cl_2/MeOH and washing with MeOH, compound **Gb-Br** (36.5 mg, 21.5 μmol) was obtained as an orange solid in a 28% yield. ^{1}H NMR (600 MHz, $CDCl_3$/TMS): δ = 8.05 (d, *J* = 8.4 Hz, 3H), 7.86 (s, 3H), 7.67 (dd, *J* = 1.8, 9.0 Hz, 3H), 7.59 (br. s, 3H), 7.51 (d, *J* = 8.4 Hz, 6H), 7.44 (d, *J* = 8.4 Hz, 6H), 7.22 (AA'BB', *J* = 9.0 Hz, 10H), 7.20 (AA'BB', *J* = 9.0 Hz, 10H), 1.34 (s, 27H); ^{13}C NMR (150 MHz, $CDCl_3$/TMS): δ = 149.9, 142.9, 140.4, 138.4, 135.0, 134.1, 132.0, 130.8. 127.0, 126.9, 125.7, 123.5, 122.1, 117.6, 111.9, 87.0, 34.5, 31.4. HR-MS (ESI, positive mode) calcd. for $[C_{86}H_{72}BBr_5N_6Ru]^+$: 1702.0884, found 1702.0856.

Ruthenium complex with X=H, R=H (Ga-H): A mixture of compound **5a** (101 mg, 0.16 mmol, 2.0 equiv.) and **6-H** (55.6 mg, 81 μmol, 1.0 equiv.) were placed in a two-necked flask. After adding anhydrous and degassed THF (4 mL), the mixture was refluxed for 119 h under N_2 atmosphere. After cooling down to room temperature, the solvent was removed by evaporation under reduced pressure. The crude product was purified by column chromatography (SiO_2, *n*-hexane/CH_2Cl_2 = 4/1). After recrystallization from CH_2Cl_2/MeOH and washing with MeOH, compound **Ga-H** (25.9 mg, 23 μmol) was obtained as an orange solid in a 28% yield. ^{1}H NMR (600 MHz, $CDCl_3$/TMS): δ = 8.07 (d, *J* = 9.0 Hz, 3H), 8.01 (s, 3H), 7.64 (dd, *J* = 1.8, 9.0 Hz, 3H), 7.55–7.54 (m, 9H), 7.41–7.38 (m, 16H), 7.28 (t, *J* = 7.5 Hz, 3H), 7.12 (t, *J* = 7.2 Hz, 5H), 7.02 (dd, *J* = 7.8, 7.8 Hz, 10H); ^{13}C NMR (150 MHz, $CDCl_3$/TMS): δ = 142.9, 141.6, 140.9, 133.8, 133.7, 133.6, 128.7, 127.2. 127.2, 127.1, 126.6, 126.5, 123.5, 118.0, 111.8, 88.0. HR-MS (ESI, positive mode) calcd. for $[C_{74}H_{53}BN_6Ru]^+$: 1138.3497, found 1138.3499.

Ruthenium complex with X=H, R=*tert*-Bu (Gb-H): A mixture of compound **5b** (101 mg, 0.13 mmol, 1.8 equiv.) and **6-H** (48.6 mg, 71 μmol, 1.0 equiv.) were placed in a two-necked flask. After adding anhydrous and degassed THF (3.2 mL), the mixture was refluxed for 5 days under N_2 atmosphere. After cooling down to room temperature, the resulting mixture was suspended in CH_2Cl_2/MeOH = 5/12 (8.5 mL) and the solid collected and washed with MeOH. The crude product was extracted with *n*-hexane (20 mL). The crude product was purified by column chromatography (SiO_2, *n*-hexane/CH_2Cl_2 = 4/1). After recrystallization from CH_2Cl_2/MeOH and washing with MeOH, compound **Gb-H** (23.7 mg, 18 μmol) was obtained as an orange solid in a 25% yield. ^{1}H NMR (600 MHz, $CDCl_3$/TMS): δ = 8.05 (d, *J* = 9.0 Hz, 3H), 7.98 (s, 3H), 7.64 (dd, *J* = 1.5, 8.7 Hz, 3H), 7.53 (br.s, 3H), 7.49 (d, *J* = 8.4 Hz, 6H), 7.42 (d, *J* = 9.0 Hz, 6H), 7.40 (d, *J* = 8.4 Hz, 10H), 7.11 (t, *J* = 7.5 Hz, 5H), 7.01 (dd, *J* = 7.8, 7.8 Hz, 10H), 1.34 (s, 27H); ^{13}C NMR (150 MHz, $CDCl_3$/TMS): δ = 149.6, 142.9, 140.8, 138.7, 134.0, 133.6, 133.6, 127.2, 127.1, 126.8, 126.4, 125.6, 123.6, 117.7, 111.8, 88.0, 34.5, 31.4. HR-MS (ESI, positive) calcd. for $[C_{86}H_{77}BN_6Ru]^+$: 1306.5379, found 1306.5199.

Electronic Supporting Information (ESI) are available with additional synthetic procedures (**4a**[33] and **4b**[34]) and all the characterizations (^{1}H NMR, ^{13}C NMR and Mass spectra for **5a**, **5b**, **Ga-Br**, **Gb-Br**, **Ga-H** and **Gb-H**). X-ray structures with ORTEP representations for **Ga-Br**, **Gb-Br**, **Ga-H** and **Gb-H** are also provided.

Deposition Numbers 2217503 (for **Ga-Br**), 2217506 (for **Gb-Br**), 2217507 (for **Ga-H**), 2217528 (for **Gb-H**) contain the supplementary crystallographic data for this paper. These data are provided free of charge by the joint Cambridge Crystallographic Data Centre and Fachinformationszentrum Karlsruhe Access Structures service.

Acknowledgements

This work has received funding from the JSPS KAKENHI grant in aid for Scientific Research on Innovative Areas "Molecular Engine (No. 8006)" 18H05419, the JSPS KAKENHI Grant-in-Aid for Challenging Research (20K21131) and the JSPS KAKENHI Grant-in-Aid for Scientific Research A (22H00325). Dr. Toshio Nishino is warmly thanked for providing the Figure 1d and Mr. Shohei Katao for his help in the single crystal XRD analysis. The University Paul Sabatier (Toulouse) and NAIST are also warmly thanked for providing a crossed position to GR.

Conflict of Interest

The authors declare no conflict of interest.

Data Availability Statement

The data that support the findings of this study are available in the supplementary material of this article.

Keywords: cyclopentadienyl ligand · indazoles · molecular gears · ruthenium · tripodal ligand

[1] M. Schliwa, *Molecular Motors*, Wiley-VCH Weinheim, **2003**.
[2] H. Noji, R. Yasuda, M. Yoshida, K. Kinosita Jr, *Nature* **1997**, *386*, 299–302.
[3] J.-P. Sauvage, *Angew. Chem. Int. Ed.* **2017**, *56*, 11080–11093; *Angew. Chem.* **2017**, *129*, 11228–11242.
[4] J. F. Stoddart, *Angew. Chem. Int. Ed.* **2017**, *56*, 11094–11125; *Angew. Chem.* **2017**, *129*, 11244–11277.
[5] B. L. Feringa, *Angew. Chem. Int. Ed.* **2017**, *56*, 11060–11078; *Angew. Chem.* **2017**, *129*, 11206–11226.
[6] a) N. Koumura, R. W. J. Zijlstra, R. A. van Delden, N. Harada, B. L. Feringa, *Nature* **1999**, *401*, 152–155; b) S. Kassem, T. van Leeuwen, A. S. Lubbe, M. R. Wilson, B. L. Feringa, D. A. Leigh, *Chem. Soc. Rev.* **2017**, *46*, 2592–2621.
[7] a) D. A. Leigh, J. K. Y. Wong, F. Dehez, F. Zerbetto, *Nature* **2003**, *424*, 174–179; b) M. von Delius, E. M. Geertsema, D. A. Leigh, *Nat. Chem.* **2010**, *2*, 96–101; c) L. Greb, A. Eichhöfer, J.-M. Lehn, *Angew. Chem. Int. Ed.* **2015**, *54*, 14345–14348; *Angew. Chem.* **2015**, *127*, 14553–14556; d) M. Guentner, M. Schildhauer, S. Thumser, P. Mayer, D. Stephenson, P. J. Mayer, H. Dube, *Nat. Commun.* **2015**, *6*, 8406; e) J. T. Foy, Q. Li, A. Goujon, J.-R. Colard-Itté, G. Fuks, E. Moulin, O. Schiffmann, D. Dattler, D. P. Funeriu, N. Giuseppone, *Nat. Nanotechnol.* **2017**, *12*, 540–545; f) V. Garcia-López, D. Liu, J. M. Tour, *Chem. Rev.* **2020**, *120*, 79–124; g) M. Baroncini, S. Silvi, A. Credi, *Chem. Rev.* **2020**, *120*, 200–268.
[8] a) T. R. Kelly, H. D. Silva, R. A. Silva, *Nature* **1999**, *401*, 150–152; b) J. V. Hernández, E. E. Kay, D. L. Leigh, *Science* **2004**, *306*, 1532–1537; c) C. Romuald, E. Busseron, F. Coutrot, *J. Org. Chem.* **2010**, *75*, 6516–6531; d) A. Goswami, S. Saha, P. K. Biswas, M. Schmittel, *Chem. Rev.* **2020**, *120*, 125–199.
[9] a) H. L. Tierney, C. J. Murphy, A. D. Jewell, A. E. Baber, E. V. Iski, H. Y. Khodaverdian, A. F. McGuire, N. Klebanov, E. C. H. Sykes, *Nat. Nanotechnol.* **2011**, *6*, 625–629; b) U. G. E. Perera, F. Ample, H. Kersell, Y. Zhang, G. Vives, J. Echeverria, M. Grisolia, G. Rapenne, C. Joachim, S.-W. Hla, *Nat. Nanotechnol.* **2013**, *8*, 46–51.
[10] a) Y. Zhang, H. Kersell, R. Stefak, J. Echeverria, V. Iancu, U. G. E. Perera, Y. Li, A. Deshpande, K.-F. Braun, C. Joachim, G. Rapenne, S.-W. Hla, *Nat. Nanotechnol.* **2016**, *11*, 706–712; b) D. Dattler, G. Fuks, J. Heiser, E. Moulin, A. Perrot, X. Yao, N. Giuseppone, *Chem. Rev.* **2020**, *120*, 310–433.
[11] a) G. Rapenne, *Org. Biomol. Chem.* **2005**, *3*, 1165–1169; b) A. A. Gakh, *Molecular Devices: An Introduction to Technomimetics and Its Biological Applications*, John Wiley & Sons, Hoboken, NJ, **2018**; c) C. Kammerer, G. Erbland, Y. Gisbert, T. Nishino, K. Yasuhara, G. Rapenne, *Chem. Lett.* **2019**, *48*, 299–308.
[12] a) T. Kudernac, N. Ruangsupapichat, M. Parschau, B. Maci, N. Katsonis, S. R. Harutyunyan, K. H. Ernst, B. L. Feringa, *Nature* **2011**, *479*, 208–211; b) J.-F. Morin, Y. Shirai, J. M. Tour, *Org. Lett.* **2006**, *8*, 1713–1716; c) H.-P. Jacquot de Rouville, R. Garbage, F. Ample, A. Nickel, J. Meyer, F.

Moresco, C. Joachim, G. Rapenne, *Chem. Eur. J.* **2012**, *18*, 8925–8928; d) T. Nishino, C. J. Martin, H. Takeuchi, F. Lim, K. Yasuhara, Y. Gisbert, S. Abid, N. Saffon-Merceron, C. Kammerer, G. Rapenne, *Chem. Eur. J.* **2020**, *26*, 12010–12018.
[13] a) Y. Gisbert, S. Abid, G. Bertrand, N. Saffon-Merceron, C. Kammerer, G. Rapenne, *Chem. Commun.* **2019**, *55*, 14689–14692; b) Y. Gisbert, C. Kammerer, G. Rapenne, *Chem. Eur. J.* **2021**, *27*, 16242–16249.
[14] Y. Gisbert, S. Abid, C. Kammerer, G. Rapenne, *Chem. Eur. J.* **2021**, *27*, 12019–12031.
[15] a) H. Iwamura, K. Mislow, *Acc. Chem. Res.* **1988**, *21*, 175–182; b) S. Toyota, T. Shimizu, T. Iwanaga, K. Wakamatsu, *Chem. Lett.* **2011**, *40*, 312–314; c) D. K. Frantz, A. Linden, K. K. Baldridge, J. S. Siegel, *J. Am. Chem. Soc.* **2012**, *134*, 1528–1535; d) H. Ube, Y. Yasuda, H. Sato, M. Shionoya, *Nat. Commun.* **2017**, *8*, 14296; e) A. Gerwien, F. Gnannt, P. Mayer, H. Dube, *Nat. Chem.* **2022**, *14*, 670–676.
[16] I. Liepuoniute, M. J. Jellen, M. A. Garcia-Garibay, *Chem. Sci.* **2020**, *11*, 12994–13007.
[17] F. Chiaravalloti, L. Gross, K.-H. Rieder, S. M. Stojkovic, A. Gourdon, C. Joachim, F. Moresco, *Nat. Mater.* **2007**, *6*, 30–33.
[18] C. Manzano, W.-H. Soe, H. S. Wong, F. Ample, A. Gourdon, N. Chandrasekhar, C. Joachim, *Nat. Mater.* **2009**, *8*, 576–579.
[19] W.-H. Soe, S. Srivastava, C. Joachim, *J. Phys. Chem. Lett.* **2019**, *10*, 6462–6467.
[20] K. H. Au Yeung, T. Kühne, F. Eisenhut, M. Kleinwächter, Y. Gisbert, R. Robles, N. Lorente, G. Cuniberti, C. Joachim, G. Rapenne, C. Kammerer, F. Moresco, *J. Phys. Chem. Lett.* **2020**, *11*, 6892–6899.
[21] a) G. Vives, H.-P. Jacquot de Rouville, A. Carella, J.-P. Launay, G. Rapenne, *Chem. Soc. Rev.* **2009**, *38*, 1551–1561; b) C. Kammerer, G. Rapenne, *Eur. J. Inorg. Chem.* **2016**, 2214–2226.
[22] a) G. Erbland, S. Abid, Y. Gisbert, N. Saffon-Merceron, Y. Hashimoto, L. Andreoni, T. Guérin, C. Kammerer, G. Rapenne, *Chem. Eur. J.* **2019**, *25*, 16328–16339; b) S. Abid, Y. Gisbert, M. Kojima, N. Saffon-Merceron, J. Cuny, C. Kammerer, G. Rapenne, *Chem. Sci.* **2021**, *12*, 4709–4721.
[23] Y. Zhang, J. P. Calupitan, T. Rojas, R. Tumbleson, G. Erbland, C. Kammerer, T. M. Ajayi, S. Wang, L. A. Curtiss, A. T. Ngo, S. E. Ulloa, G. Rapenne, S.-W. Hla, *Nat. Commun.* **2019**, *10*, 3742.
[24] Molecular modellings were performed using Spartan Student Edition V7 based on the crystal structure of analog complexes bearing this tripodal ligand.[13a].
[25] a) S. Trofimenko, *Scorpionates : The Coordination Chemistry of Polypyrazolylborate Ligands*, Imperial College Press, London, **1999**; b) S. Trofimenko, *Chem. Rev.* **1993**, *93*, 943–980.
[26] a) A. L. Rheingold, B. S. Haggerty, G. P. A. Yap, S. Trofimenko, *Inorg. Chem.* **1997**, *36*, 5097–5103; b) C. Janiak, S. Temizdemir, S. Dechert, *Inorg. Chem. Commun.* **2000**, *3*, 271–275; c) A. Carella, G. Vives, T. Cox, J. Jaud, G. Rapenne, J.-P. Launay, *Eur. J. Inorg. Chem.* **2006**, 980–987.
[27] B. Martín-Matute, M. Edin, K. Bogár, F. B. Kaynak, J.-E. Bäckvall, *J. Am. Chem. Soc.* **2005**, *127*, 8817–8825.
[28] A. Carella, R. Poteau, G. Rapenne, J.-P. Launay, *Chem. Eur. J.* **2008**, *14*, 8147–8156.
[29] G. M. Sheldrick, *Acta Cryst. Sect. A* **2015**, *71*, 3–8.
[30] G. M. Sheldrick, *Acta Cryst. Sect. C* **2015**, *71*, 3–8.
[31] O. V. Dolomanov, L. J. Bourhis, R. J. Gildea, J. A. K. Howard, H. Puschmann, *J. Appl. Crystallogr.* **2009**, *42*, 339–341.
[32] C. Lopez, R. M. Claramunt, D. Sanz, C. F. Foces, F. H. Cano, R. Faure, E. Cayon, J. Elguero, *J. Inorg. Chim. Acta* **1990**, *176*, 195–204.
[33] L. Rooney, A. Vidal, A.-M. D'Souza, N. Devereux, B. Masick, V. Boissel, R. West, V. Head, R. Stringer, J. Lao, M. J. Petrus, A. Patapoutian, M. Nash, N. Stoakley, M. Panesar, J. M. Verkuyl, A. M. Schumacher, H. M. Petrassi, D. C. Tully, *J. Med. Chem.* **2014**, *57*, 5129–5140.
[34] F. Song, G. Xu, M. D. Gaul, B. Zhao, T. Lu, R. Zhang, R. L. DesJarlais, K. DiLoreto, N. Huebert, B. Shook, D. Rentzeperis, R. Santulli, A. Eckardt, K. Demarest, *Bioorg. Med. Chem. Lett.* **2019**, *29*, 1974–1980.

Manuscript received: November 9, 2022
Accepted manuscript online: January 25, 2023
Version of record online: March 1, 2023

Correction added on March 9, 2023, after first online publication: comments that were incorrectly introduced during the proofs stage in the captions of Figures 1, 6, and Table 1 have been removed.